

Nanoscale

Accepted Manuscript



This is an *Accepted Manuscript*, which has been through the Royal Society of Chemistry peer review process and has been accepted for publication.

Accepted Manuscripts are published online shortly after acceptance, before technical editing, formatting and proof reading. Using this free service, authors can make their results available to the community, in citable form, before we publish the edited article. We will replace this *Accepted Manuscript* with the edited and formatted *Advance Article* as soon as it is available.

You can find more information about *Accepted Manuscripts* in the [Information for Authors](#).

Please note that technical editing may introduce minor changes to the text and/or graphics, which may alter content. The journal's standard [Terms & Conditions](#) and the [Ethical guidelines](#) still apply. In no event shall the Royal Society of Chemistry be held responsible for any errors or omissions in this *Accepted Manuscript* or any consequences arising from the use of any information it contains.

Self-interconnecting Pt Nanowire Network Electrode for Electrochemical Amperometric Biosensor

Cite this: DOI: 10.1039/x0xx00000x

Shuqi Wang,^{a,b} Li-Ping Xu,^{*a,b} Hai-Wei Liang,^d Shu-Hong Yu,^{*d} Yongqiang Wen,^{a,b} Shutao Wang^{*c} and Xueji Zhang^{*a,b}

Received 00th January 2012,
Accepted 00th January 2012

DOI: 10.1039/x0xx00000x

www.rsc.org/

One-dimensional Pt nanostructures are of considerable interest for the development of highly stable and sensitive electrochemical sensors. This paper described a self-interconnecting Pt nanowire network electrode (PtNNE) for detection of hydrogen peroxide (H_2O_2) and glucose with ultrahigh sensitivity and stability. The as-prepared PtNNE consists of polycrystalline nanowires with high-index facets along the side surface which providing more active surface atoms on kinks and steps, and those ultralong nanowires interconnected with each other to form a free-standing network membrane. The excellent structure features of PtNNE promoted the performance of Pt-based electrochemical sensor both in electrocatalytic activity and stability. Amperometric measurements towards hydrogen peroxide were performed, the PtNNE sensor showed an extremely high sensitivity of $1360 \mu\text{A mM}^{-1} \text{cm}^{-2}$. This excellent sensitivity mainly attributes to the high-index facets of nanowires superior electrocatalytic activity towards H_2O_2 and the interconnected nanowire network formed “electron freeway” transport model, which could provide multiple electron pathways and fast electron transport on the electrode, leading to rapid reaction and sensitive signal detection. The as-prepared PtNNE also hold promise in oxidase based biosensor. As a proof of concepts, PtNNE based glucose biosensor also showed an outstanding sensitivity as high as $114 \mu\text{A mM}^{-1} \text{cm}^{-2}$, a low detection limit of $1.5 \mu\text{M}$, and an impressive detection range from $5 \mu\text{M}$ to 30mM .

Introduction

The level of hydrogen peroxide (H_2O_2) has been suggested as a potential biomarker of whole body oxidative stress.¹⁻³ H_2O_2 is also always concerned in various fields such as food processes, textile industry, pulp and paper bleaching, pharmaceutical research, etc.⁴⁻⁷ Therefore, the development of hydrogen peroxide sensors with high sensitivity and high stability is not only of practical significance for point-of-care detection, but also important for academic and industrial purposes. For decades, electrochemical (EC) based H_2O_2 sensors have attracted much attention due to their merits of providing an accurate, sensitive and yet simple, inexpensive, compact and low-power platform for on-site detecting.⁸ Moreover, since H_2O_2 is an important product in oxidase reaction, EC-based H_2O_2 sensors have been intensely applied to fabricate oxidase-based biosensor, especially for glucose oxidase biosensor which is of great demand in the clinical applications about diabetes and endocrine metabolic disorder diagnosis.⁹ Hence, it is highly desirable to develop either H_2O_2 or glucose biosensors with excellent and stable performance.

Owing to the booming development in nanotechnology and the outstanding chemical/physical properties of nanomaterials, the electrochemical sensor performance has been remarkably enhanced, which could make the electrochemical devices meet the urgent need of biomedical and environmental applications.¹⁰⁻¹² Platinum (Pt) based nanomaterials have been widely employed in the detection of H_2O_2 and glucose due to their excellent electrocatalytic capability for the oxidation and reduction of H_2O_2 .¹³⁻¹⁵ The greatly enhanced electrocatalytic activity of Pt nanomaterials mainly attributes to their enlarged surface area and favorable lattice planes which provide enormous number of active centers for electrochemical reactions and facilitate the electron transfer reaction of H_2O_2 .^{16, 17} The most widely studied electrocatalyst is Pt nanoparticles (Pt NPs) which were often dispersed on support materials with large surface area.^{12, 18-20} Although Pt NPs can achieve high electrocatalytic activity, their applications are restricted by their poor durability. The electrochemical reaction and Ostwald ripening may lead to the migration and coalescence of Pt NPs, and ultimately result in the detachment of Pt NPs from the electrodes.^{21, 22} Moreover, the poor connection at the interface between nanoparticles and support materials may impede mass

diffusion, and result in a large resistance for the electron transfer.²³ In contrast to Pt nanoparticles, one-dimensional (1D) Pt nanomaterials such as Pt nanowires exhibit high stability, easy electron transport and high electrocatalytic activity due to their anisotropy, unique structure or surface properties.^{24, 25} Pt nanowires have adequate active facets exposing on their large side surface and provide the facile pathways for the electron transfer by reducing the number of interfaces between the nanoparticles.^{26, 27} Hence, Pt nanowires would be a very promising electrode in electrochemical sensors. Several studies demonstrated that H₂O₂ electrochemical sensors based Pt nanowires exhibited obvious improvements in sensitivity and durability.²⁸⁻³⁰ However, currently most Pt nanowires were still in the form of powder and the discontinuity of nanowires may make the prepared electrode less stable and less conductive.

Three-dimensional (3D) conducting network provides a rational solution to improve the electronic conductivities of nanomaterials. The assembly of 1D nanomaterials into 3D macroscopic membranes is highly desired because these nanofibrous membranes possess good flexibility, high stability, interconnected nanowire network and high porosity and large specific surface area.^{31, 32} In this work, a self-interconnecting Pt nanowire network electrode (PtNNE) was prepared.³³ Due to its intrinsic nanostructure, the as-prepared PtNNE showed an excellent performance in electrocatalysis of oxygen. Our results indicated that the self-interconnecting PtNNE showed a greatly enhanced sensitivity and stability towards H₂O₂ electrocatalysis, and also hold the promise for sensitive detection of glucose in oxidase enzyme based biosensor.

Experimental

Reagents

Hydrogen peroxide (H₂O₂) was stored at 4 °C and diluted to required concentrations before use. H₂O₂, glutaraldehyde (50%), D-(+)-glucose (99.5%) were obtained from Sinopharm Chemical Reagent Co., Ltd., China. Dihydrogen hexachloroplatinate hexahydrate (H₂PtCl₆ · 6H₂O) was obtained from Alfa Aesar. L-ascorbic acid (AA), uric acid (UA), Dopamine (DA) and glucose oxidase (GOx, from *Aspergillus niger*, EC 1.1.3.4, 50 KU) were all provided by Sigma-Aldrich. All other reagents were commercially available and of analytical reagent grade. All solutions were prepared with ultrapure water (Milli-Q, 18.2 MΩ cm).

Instruments

The scanning electron microscope (SEM) images and the energy dispersive X-ray (EDX) spectroscopy analysis were obtained with a JEOL JSM-6701F (JEOL, Japan). Transmission electron microscope (TEM) measurements were performed on TECNAL G2 F30 S-TWIN (FEI, USA) operated at an acceleration voltage of 300 kV. Atomic force microscope (AFM) images were obtained on a Bruker Nanoscope IIIa. Fourier transform infrared (FT-IR) spectra by KBr containing the PtNNE/GOx were carried out on a Thermo Nicolet 6700 FT-IR spectrometer at room temperature. Electrochemical measurements were performed using a 660D Electrochemical

Analyzer (CHI Instrument Inc., USA). The X-ray diffraction (XRD) analyses were carried out using PANalytical Empyrean X-ray diffractometer with CuKα radiation. Electrochemical impedance spectroscopy (EIS) measurements were carried out with an Autolab PGSTAT 302N (Metrohm, Switzerland) and the frequency range was at 0.1 Hz–100 kHz at 210 mV vs. Ag/AgCl.

Fabrication of Self-interconnecting PtNNE

Te nanowire and Te@C nanocables templates was firstly synthesized via a simple hydrothermal method and the procedures were well described in previous work.^{34, 35} In brief, Te nanowire was dispersed into 0.35 mol/L glucose solution with magnetic stirring for 15 min, then the hydrothermal carbonization process was carried out at 160 °C for 18 hours. The as-prepared Te@C nanocables were washed with absolute ethanol and ultrapure water, then 0.2 mM H₂PtCl₆ was mixed and shaken reacting at 50 °C for 12 hours. The Pt@C nanowires were collected with ultrapure water by filtration, and then redispersed in ethanol under vigorous stirring for 3 hours.³⁶ The suspension was poured into a container to evaporate for one day at room temperature. Finally, the self-interconnecting Pt nanowire membrane could be obtained by calcination of Pt@C nanocable membrane at 400 °C for 1 hour.³³

A glassy carbon electrode (GCE, 3 mm in diameter, area ~ 0.07 cm²) served as the substrate for the working electrode. Prior to use, the GCE was first polished with 0.3 and 0.05 μm alumina slurry on felt polishing pads, and cleaned with ultrasonication in ethanol and water successively, and then dried under a nitrogen stream. A round as-prepared PtNNE (~3 mm in diameter) was adhered on the GCE using Nafion solution (5 μL, 0.05 wt%).

Immobilization of GOx on PtNNE

Before immobilization of GOx, PtNNE was electrochemically cleaned by cyclic voltammetry in 0.5 M H₂SO₄ solution to produce a clean electrode surface, which was followed with rinsing using water and PBS, then dried under a nitrogen stream. The GOx was dissolved into 0.1 M PBS (pH 7.0) with a final concentration of 20 mg/ml. Then 10 μL of the GOx solution was dropped onto PtNNE surface, and maintained under room temperature until dry. Subsequently, 10 μL of 2.5% glutaraldehyde was then dropped onto the surface of the electrode, and reacted for 4 h to cross-link GOx with the PtNNE. Finally, the modified electrode was washed thoroughly with PBS in order to remove unfixed molecules. The PtNNE/GOx was stored in PBS at room temperature before use.

Electrochemical Measurements

All the electrochemical measurements were performed in a three-electrode system. The as-prepared PtNNE used as working electrode, Ag/AgCl and platinum wire were used as reference and counter electrodes, respectively. Before electrochemical measurements, the PtNNE was first cycled from -0.2 V to -1.2 V versus Ag/AgCl at 100 mV/s in 0.5 M

H₂SO₄ solution to produce a clean electrode surface. All amperometric measurements were implemented by successive addition of analytes into 0.1 M PBS (pH 7.0) with a constant stir at room temperature.

Results and Discussion

Synthesis of Self-interconnecting PtNNE and Structural Characterization

The self-interconnecting Pt nanowire network electrode (PtNNE) was fabricated via a multiplex templating process. Ultrathin Te nanowire was synthesized firstly via a simple hydrothermal method. Then by hydrothermal carbonization of glucose on Te nanowire, Te@C nanocables were prepared successfully. Through a redox reaction between H₂PtCl₆ and Te, Pt@C nanocables were obtained on the Te@C nanocables template. Pt@C nanocable assembled into a free-standing membranes by a solvent-evaporation-induced self-assembly process.³⁴⁻³⁶ Finally, the self-interconnecting PtNNE obtained by calcination of Pt@C nanocable membranes at 400 °C in air for 1 h to remove the carbon species. The X-ray diffraction (XRD) and energy dispersive X-ray (EDX) spectrum (shown in Supporting Information, Fig. S1.) displayed the typical diffractions peaks of Pt, confirming that the final products consisted exclusively of Pt element.

Scanning electron microscopy (SEM) and transmission electron microscopy (TEM) images (Fig. 1A–C) showed that the as-prepared PtNNE have very fine wire-like nanostructures with lengths of several tens of micrometers and diameter of about 12 nm. Side-view SEM images (Fig. 1B and Fig. S2.) revealed that those high-aspect-ratio Pt 1D nanowires interconnected with each other to form a highly porous nanowire network membrane with a thickness of about 6 μm. The nanowire network exhibited a good stability that nanowire entangled with each other even after ultrasonic treatment (Fig.

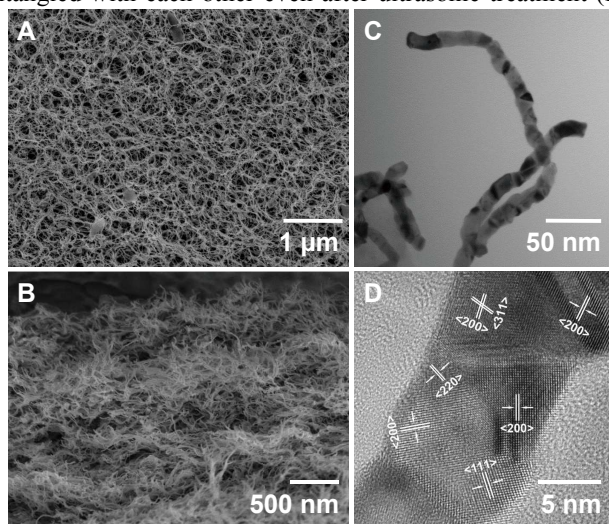


Fig. 1. The SEM and TEM images of PtNNE. (A) Top-view and (B) side-view SEM images of self-interconnecting PtNNE. (C) TEM images of Pt nanowires dispersed by ultrasonic treatment. (D) High-magnification TEM image of Pt nanowire showing crystalline lattice fringes recorded from (C).

S2A). This porous structure could provide large amount of surface areas and abundant active sites, also could facilitate electron transport and reagent diffusion on the electrode, which is crucial for electrocatalytic reactions in electrochemical sensor application.¹⁶ Furthermore, TEM images in Fig. 1C, D revealed that the single Pt nanowire was composed of multiple single-crystal facets on its side surface extending along the axis of the nanowire. The observed (111), (200), (220) and (311) crystal planes of pure Pt with face-centered-cubic (fcc) phase (JCPDS 04-802) were in good agreement with their characteristic peaks in XRD spectrum, (222) crystal plane was also found in XRD spectrum. It was reported that the polycrystalline Pt 1D nanowire with high-index facets exhibited superior electrocatalytic active due to their high percentage of surface atoms located at steps and kinks.³⁷⁻³⁹ Hence, the self-interconnecting Pt nanowire network with porous structure and high-index facets hold the promise as electrochemical sensor with high performance.

The electrochemical properties of PtNNE were characterized by cyclic voltammetry (CV) and electrochemical impedance spectroscopy (EIS). The estimating the

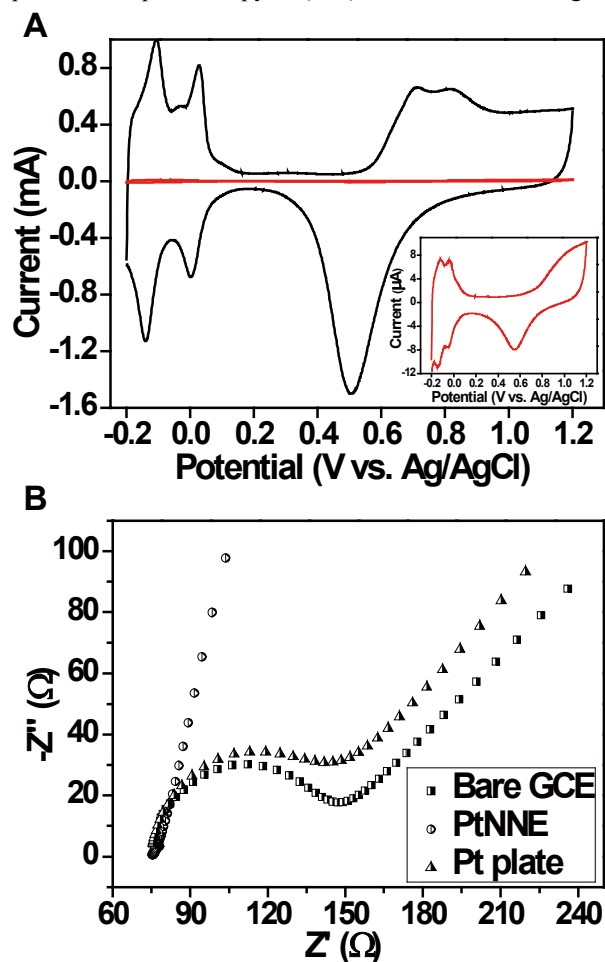


Fig. 2. (A) Cyclic Voltammograms obtained at PtNNE (black line) and Pt plate electrode (red line) in N₂-saturated 0.5 M H₂SO₄ at 50 mV/s. The inset shows the enlarged CV of Pt plate electrode. (B) Nyquist plots of 5 mM [Fe(CN)₆]^{3-/4-} obtained at bare GCE, PtNNE and Pt plate electrode.

electrochemical active surface area (ECSA) is a critical performance metric for catalyst and membrane electrode, and the technique of using a hydrogen adsorption/desorption method in conjunction with cyclic voltammetry has been used for several decades.^{40, 41} The cyclic voltammogram of PtNNE and a commercial Pt plate electrode (for comparison) were scanned in deaerated H₂SO₄ solutions within a potential range from -0.2 to 1.2 V as shown in Fig. 2A. PtNNE exhibited well-defined hydrogen adsorption/desorption peaks, which attributed to the different crystal facets of polycrystalline Pt 1D nanostructure. ECSA was calculated by integrating the charge associated with hydrogen adsorption/desorption region, and assuming 210 $\mu\text{C cm}^{-2}$ for the adsorption of a monolayer of hydrogen on a Pt surface. The electrochemical active surface area of PtNNE was determined to be 15.15 cm², which is almost 214 times of its projected area (the projected area refers to its geometric area). In contrast, the electrochemical active surface of commercial Pt plate electrode is about 0.11 cm² (calculated from CV in Fig. 2A), which is 1.5 times of its projected area. This result indicated that the surface area of PtNNE was highly increased by the fine wire-like nanostructures.

EIS is an effective approach to analyze the interfacial properties of electrodes. A typical impedance spectrum (Nyquist plot) includes a semicircle portion at higher frequencies and a linear part at lower frequency range. They represent the electron-transfer-limited process and the diffusion limited process respectively. The semicircle diameter in the impedance spectra equals to the electron-transfer resistance (R_{et}), which determines the electron-transfer kinetics of the redox probe at the electrode interface.³⁰ Fig. 2B showed the Nyquist plots of PtNNE, bare GCE and commercial Pt plate electrode in 5 mM [Fe(CN)₆]^{3-/4-}. It can be seen that a semicircle curve were obtained with the bare GCE and commercial Pt plate electrode, which indicated a slow electron transfer process. As for PtNNE, the curve was almost a straight line, which implied a diffuse limiting step of the electrochemical processes and indicated that PtNNE promoted the electron transfer of the electrochemical probe. Based on above analysis, the large active surface areas (ECSA) and the enhanced electron transfer properties of PtNNE definitely lead to the enhanced electrocatalytic activities.

Electrocatalytic Performances of PtNNE towards H₂O₂

Amperometric responses of PtNNE towards successive injection of different concentration of H₂O₂ were measured at the optimized potential of 0 V under a constant stirring condition (see supplementary information and Fig. S3, Fig. S4), and the typical current-time curves were showed in Fig. 3A. Pt plate electrode was also evaluated for comparison. PtNNE showed a very fast response toward H₂O₂ and could achieve the maximum steady-state current within 3 s, which indicated that PtNNE has high electrocatalytic efficiency toward reduction of H₂O₂. The electrocatalytic properties of PtNNE were demonstrated clearly in the calibration plot of steady-state

currents against the concentration of H₂O₂ in Fig. 3B. The current responses increased linearly with increasing of H₂O₂ concentration in the range of 5 μM –3 mM with a correlation coefficient of 0.999, a detection limit of 9.6 μM was obtained (based on signal-to-noise ratio, S/N = 3). Noticeably, PtNNE displayed a remarkable sensitivity as high as 1360 $\mu\text{A mM}^{-1} \text{cm}^{-2}$ (based on its geometric cross-sectional area), which was much higher than that of Pt plate electrode (282 $\mu\text{A mM}^{-1} \text{cm}^{-2}$). The reported highest sensitivity of other Pt based H₂O₂ electrocatalytic electrode is about 900 $\mu\text{A mM}^{-1} \text{cm}^{-2}$.^{17, 29, 30, 42-44} Hence, the as-prepared PtNNE displayed an outstanding sensitivity.

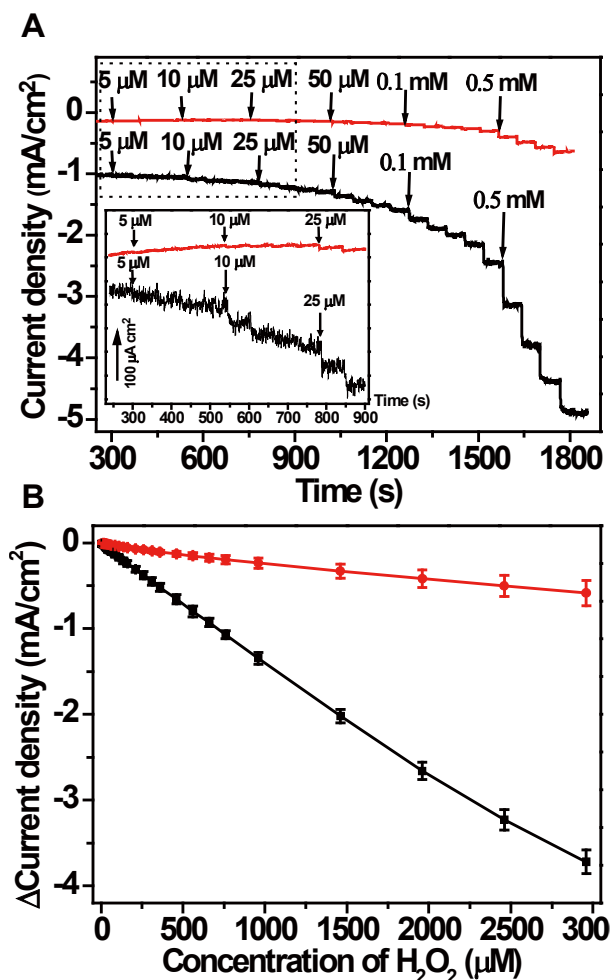
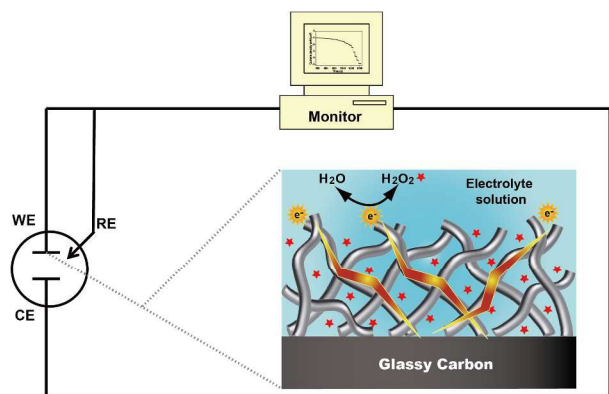


Fig. 3. (A) Amperometric responses of PtNNE (black line) and Pt plate electrode (red line) to successive injection of different concentration of H₂O₂ into a stirred solution of 0.1 M PBS (pH 7.0) at applied potential of 0 V. The inset was the amperometric responses at the region of low concentration (dash box). (The current density was calculated by the projected area) (B) The calibration curve plots for H₂O₂ responses of PtNNE (black line) and Pt plate electrode (red line). For PtNNE, linear range is 5 μM ~ 3 mM, $y = -0.0031 - 0.00136x$, $r = 0.999$ ($x/\mu\text{M}$, $y/\text{mA cm}^{-2}$). For Pt plate electrode, $y = -0.00226 - 0.000282x$, $r = 0.9436$. Error bars represent the standard deviations of three independent measurements

The extraordinary electrocatalytic activity towards H_2O_2 and high sensitivity of PtNNE mainly attribute to the self-intercrossing 3D nanowire network structure of PtNNE membrane. Firstly, Pt nanowire network structure has large surface areas as discussed previously (Fig. 2A), which provides sufficient contacting area for analyte with electrode and also abundant electroactive sites for efficient electrocatalytic reactions. Secondly, the as-prepared Pt nanowires are bounded by high-index facets, which have high percentage of surface atoms located at steps and kinks, displaying superior electrocatalytic activity to that of the flat planes for several reactions such as electroreduction of O_2 , which is also highly active for reduction of H_2O_2 (H_2O_2 is an intermediate product of O_2 reduction).³⁹ Moreover, the poriferous network facilitates electrolyte and analyte transport and gas diffusion on the electrode, which is beneficial for electrocatalytic reaction. Most importantly, 1D Pt nanowires formed the self-interconnecting network spontaneously without adding any extra binders. The pure PtNNE was convinced to have high conductivity (Fig. 2B). Thus PtNNE makes the electrons transfer easier and provides multiple effective electron transport pathways as shown in Scheme 1, leading to rapid reaction and sensitive signal detection.



Scheme 1. Multiple effective pathways for electron transporting of PtNNE.

Considering its practical application, the reproducibility of PtNNE was also examined by successive measurements of $100 \mu\text{M}$ H_2O_2 by the same sensor. The relative standard deviation (RSD) in response to 10 measurements by the same electrode was 4.5%. The good reproducibility implied the reliability of the electrode for detection of H_2O_2 . PtNNE was stored at room temperature in PBS (pH 7.0) for one month, the current responses to $100 \mu\text{M}$ H_2O_2 remained 97% of its original value (Fig. 4), which showed satisfactory long-term stability of PtNNE. The stability of response signal indicated that PtNNE was very stable, which attributed to unique self-interconnecting network structure formed by nanowires. The selected detection potential ensured the good selectivity of the sensor in the presence of common interferences and oxygen. Therefore, the as-prepared PtNNE could be a promising electrode material for preparation of sensitive and stable amperometric sensors toward H_2O_2 detecting.

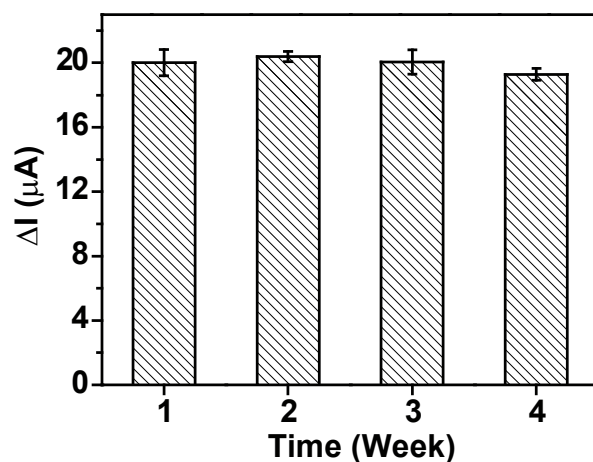


Fig. 4. Long-term stability of PtNNE in response to $100 \mu\text{M}$ H_2O_2 .

PtNNE/GOx Glucose Biosensor Performance

The self-interconnecting PtNNE holds the promise of application in a number of oxidase-based amperometric biosensors. As for an example, experiment with glucose oxidase based PtNNE was further carried out for glucose detection. GOx was successfully immobilized on PtNNE according to the atomic force microscope (AFM) images and Fourier transform infrared (FT-IR) spectra (Fig. S5 and S6). The measurement of glucose relied on detection of hydrogen peroxide produced by the reduction of oxygen during glucose oxidase reaction. According to previous studies (Fig. S4), glucose could be directly oxidized by bare Pt electrode in the range of $-0.3 \sim 0.1$ V, hence the reduction potential of 0 V for H_2O_2 detection was not suitable for glucose detection. Based on the current responses of PtNNE towards 1 mM H_2O_2 at different applied potential in Fig. S7A, the measurements of glucose were carried out at an optimally sensitive potential of $+0.6$ V vs. Ag/AgCl, which was also consistent with the literatures.^{9, 45} Fig. 5A showed the typical amperometric responses of the PtNNE/GOx with successive addition of glucose. The current increased and quickly reached a steady-state (5–10 s) with increasing the glucose concentration, and current responses were obtained for different concentrations of glucose. It could be seen from the calibration curve in Fig. 5B that the PtNNE/GOx displayed an outstanding performances which involved two main points: 1) the extremely high sensitivity toward glucose, the detection limit was obtained to be $1.5 \mu\text{M}$ (based on signal-to-noise ratio $S/N = 3$) and the sensitivity in the linear range was calculated to be as high as $114 \mu\text{A mM}^{-1} \text{ cm}^{-2}$, which was much higher than most previous enzyme biosensors based on Pt.^{30, 46} 2) A excellent linear range from $5 \mu\text{M}$ to 30 mM with a correlation coefficient of 0.995. When glucose concentration exceeded 30 mM , the current responses slightly began to deviate from linearity because of the oxygen dependence of GOx based biosensors. Obviously, this extensive detection range is superior to previously reported Pt glucose sensors.

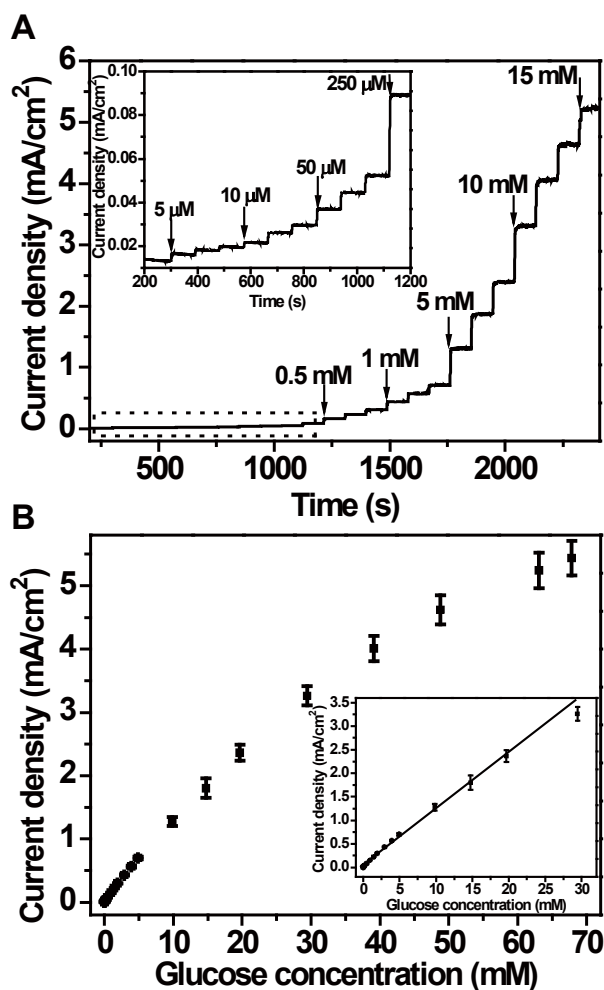


Fig. 5. (A) Amperometric responses of PtNNE/GOx with successive addition of various concentrations of glucose at 0.1 M PBS at an applied potential of 0.6 V vs. Ag/AgCl. Inset shown the magnified part of the curve marked with the dash square. (B) The calibration curves according to (A) for glucose concentrations from 5 μM to 70 mM. The inset shown the fitting straight-line for lower concentration from 5 μM to 30 mM, $y = 0.114x + 0.046$, (x/mM , $y/\text{mA cm}^{-2}$). Error bars represent the standard deviations of three independent measurements.

PtNNE played an important role as both the enzyme loading support and the excellent electrocatalyst for this enhanced performance of glucose sensor. The poriferous nanowire network allowed the efficient immobilization of enzyme on the side surface of nanowires, providing a short diffusion pathway for H_2O_2 reaction. The fast response and the sensitive signal demonstrated that H_2O_2 produced near GOx could be directly catalyzed by the interconnecting PtNNE nearby. Additionally, the interconnecting PtNNE facilitated the diffusion of electrolyte, glucose and O_2 on the electrode, which providing the sufficient area for interfacial reaction. With the successfully fabricated high performance of H_2O_2 and glucose biosensor, the proposed interconnecting PtNNE could be very promising in other oxidase-based sensor.

The selectivity of the PtNNE/GOx biosensor was investigated. The common interfering substances of ascorbic

acid (AA) and uric acid (UA) were added into glucose detection in Fig. S7B. The current responses upon 0.5 mM UA and 1 mM AA were 0.4% and 7.3% of that to 5 mM glucose, respectively, which indicating a good selectivity.

The reproducibility is important in evaluating the performance of biosensors. The amperometric responses of 1 mM glucose for 8 times using the sample PtNNE/GOx were carried out in Fig. S8. A relative standard deviation (RSD) of 4.1% signal changes was obtained, which indicated the good repeatability of this biosensor. Moreover, the electrode-to-electrode reproducibility was studied by measurement of four independently prepared PtNNE/GOx biosensors. A RSD of 3.5% (responses to 1 mM glucose) was obtained, representing a good reproducibility of the biosensor.

To evaluate the practical application of the biosensor, simulative blood sample (0.1 M PBS, pH 7.4, containing 0.1 mM AA, 0.1 mM DA, 0.02 mM UA and 0.15 mM chloride ions) and fetal calf serum (containing various proteins, 1:10 diluted with 0.1 M PBS, pH 7.0) were used as electrolyte to detect glucose.^{42, 47} The amperometric responses to 1 mM glucose in such simulative blood and serum samples were about 99% and 94% of that in PBS, respectively, which indicated the less influence on glucose detection. All the above results revealed the potential application in glucose biosensor.

Conclusions

In summary, we have demonstrated a three-dimensionally self-interconnecting Pt nanowire network electrode platform for ultrahigh sensitive detection of H_2O_2 and glucose. The PtNNE was fabricated via a simply step-by-step multi-templating process. The as-prepared PtNNE showed an outstanding sensitivity and a satisfactory long-term stability towards H_2O_2 detection. The excellent electrocatalytic sensitivity of PtNNE mainly attributed to its unique structure determined enhancements, i.e. the porous structure provided the greatly enlarged surface active area and enhanced mass transportation and gas diffusion; and then the 1D formed 3D pure Pt nanowire network structure owned the high stability and very fast electron transfer property, which could largely reducing the interfacial resistance comparing with that of hybrid Pt nanomaterials. The PtNNE was also applied to fabricate the GOx-based glucose biosensor. As a result, it showed a low detection limit of 1.5 μM , a high sensitivity of $114 \mu\text{A mM}^{-1} \text{cm}^{-2}$, and a considerably wide detection range from 5 μM to 30 mM. The present results suggested that the as-prepared Pt nanowire electrode with interconnecting network structure can serve as a promising electrochemical platform for a number of oxidase-based enzymes biosensors.

Acknowledgements

The work was supported by National Natural Science Foundation of China (NSFC Grant No. 21475009, 2012CB933800, 21175140, 21073203, 21127007, 21275017, 91227103), the Fundamental Research Funds for the Central

Universities (FRF-TP-14-065A2) and Beijing Higher Education Young Elite Teacher Project (YETP0424).

Notes and references

^a Research Center for Bioengineering and Sensing Technology, University of Science & Technology Beijing, Beijing 100083, P.R. China. Fax: 86-10-82375840; Tel: 86-10-82375840; E-mail: xuliping@ustb.edu.cn; stwang@mail.ipc.ac.cn; zhangxueji@ustb.edu.cn.

^b School of Chemistry and Biological Engineering, University of Science and Technology Beijing, Beijing, 100083, P.R. China.

^c Laboratory of Bioinspired Smart Interface Science, Technical Institute of Physics and Chemistry, Chinese Academy of Sciences, Beijing 100190, P.R. China.

^d Division of Nanomaterials and Chemistry, Hefei National Laboratory for Physical Sciences at Microscale, Department of Chemistry, the National Synchrotron Radiation Laboratory, University of Science and Technology of China, Hefei, Anhui 230026, P.R. China.

† Electronic Supplementary Information (ESI) available: EDS spectrum and XRD pattern of PtNN membrane; High-magnification side-view SEM images of PtNNE; Cyclic voltammogram (CV) of PtNNE in response to H₂O₂ and current responses of 200 μM H₂O₂ at different applied potentials; Amperometry responses of PtNNE towards common endogenous electroactive interferences at different potential. Amperometry responses of PtNNE/Gox upon common interferences. See DOI: 10.1039/b000000x/

- R. Stocker and J. F. Keaney, *Physiol. Rev.*, 2004, **84**, 1381-1478.
- U. Singh and I. Jialal, *Pathophysiology*, 2006, **13**, 129-142.
- M. Lopez-Lazaro, *Cancer Lett.*, 2007, **252**, 1-8.
- C. Brandt and R. van Eldik, *Chem. Rev.*, 1995, **95**, 119-190.
- K. Kriz, M. Anderlund and D. Kriz, *Biosens. Bioelectron.*, 2001, **16**, 363-369.
- T. M. Schreier, J. J. Rach and G. E. Howe, *Aquaculture*, 1996, **140**, 323-331.
- Y. Wang, J. Huang, C. Zhang, J. Wei and X. Zhou, *Electroanalysis*, 1998, **10**, 776-778.
- J. Wang, *Analyst*, 2005, **130**, 421-426.
- A. Heller and B. Feldman, *Chem. Rev.*, 2008, **108**, 2482-2505.
- S. Wang, L.-P. Xu, Y. Wen, H. Du, S. Wang and X. Zhang, *Nanoscale*, 2013, **5**, 4284-4290.
- L.-P. Xu, S. Wang, H. Dong, G. Liu, Y. Wen, S. Wang and X. Zhang, *Nanoscale*, 2012, **4**, 3786-3790.
- C. Yang, M. Zhou and Q. Xu, *Nanoscale*, 2014, **6**, 11863-11870.
- S. B. Hall, E. A. Khudaish and A. L. Hart, *Electrochim. Acta*, 1998, **43**, 2015-2024.
- I. Katsounaros, W. B. Schneider, J. C. Meier, U. Benedikt, P. U. Biedermann, A. A. Auer and K. J. Mayrhofer, *Phys. Chem. Chem. Phys.*, 2012, **14**, 7384-7391.
- L. Qiang, S. Vaddiraju, D. Patel and F. Papadimitrakopoulos, *Biosens. Bioelectron.*, 2011, **26**, 3755-3760.
- A. Chen and P. Holt-Hindle, *Chem. Rev.*, 2010, **110**, 3767-3804.
- F. Xiao, Y. Li, X. Zan, K. Liao, R. Xu and H. Duan, *Adv. Funct. Mater.*, 2012, **22**, 2487-2494.
- S. Hrapovic, Y. Liu, K. B. Male and J. H. T. Luong, *Anal. Chem.*, 2003, **76**, 1083-1088.
- J.-M. You, D. Kim and S. Jeon, *Electrochim. Acta*, 2012, **65**, 288-293.
- T.-Y. Jeon, N. Pinna, S. J. Yoo, D. Ahn, S. H. Choi, M.-G. Willinger, Y.-H. Cho, K.-S. Lee, H.-Y. Park, S.-H. Yu and Y.-E. Sung, *Nanoscale*, 2012, **4**, 6461-6469.
- P. J. Ferreira, G. J. la O', Y. Shao-Horn, D. Morgan, R. Makharia, S. Kocha and H. A. Gasteiger, *J. Electrochem. Soc.*, 2005, **152**, A2256-A2271.
- X. Yu and S. Ye, *J. Power Sources*, 2007, **172**, 133-144.
- S. Wang, S. P. Jiang, T. J. White, J. Guo and X. Wang, *J. Phys. Chem. C*, 2009, **113**, 18935-18945.
- C. Koenigsmann, M. E. Scofield, H. Liu and S. S. Wong, *J. Phys. Chem. Lett.*, 2012, **3**, 3385-3398.
- M. Rauber, I. Alber, S. Müller, R. Neumann, O. Picht, C. Roth, A. Schökel, M. E. Toimil-Molares and W. Ensinger, *Nano Lett.*, 2011, **11**, 2304-2310.
- B. Wang, S. Yin, G. Wang, A. Buldum and J. Zhao, *Phys. Rev. Lett.*, 2001, **86**, 2046-2049.
- S. Wang, S. P. Jiang, X. Wang and J. Guo, *Electrochim. Acta*, 2011, **56**, 1563-1569.
- J. J. Wang, N. V. Myung, M. H. Yun and H. G. Monbouquette, *J. Electroanal. Chem.*, 2005, **575**, 139-146.
- M. Yang, F. Qu, Y. Lu, Y. He, G. Shen and R. Yu, *Biomaterials*, 2006, **27**, 5944-5950.
- Y. Wang, Y. Zhu, J. Chen and Y. Zeng, *Nanoscale*, 2012, **4**, 6025-6031.
- Y. Xia, P. Yang, Y. Sun, Y. Wu, B. Mayers, B. Gates, Y. Yin, F. Kim and H. Yan, *Adv. Mater.*, 2003, **15**, 353-389.
- J.-W. Liu, H.-W. Liang and S.-H. Yu, *Chem. Rev.*, 2012, **112**, 4770-4799.
- H.-W. Liang, X. Cao, F. Zhou, C.-H. Cui, W.-J. Zhang and S.-H. Yu, *Adv. Mater.*, 2011, **23**, 1467-1471.
- H.-S. Qian, S.-H. Yu, J.-Y. Gong, L.-B. Luo and L.-f. Fei, *Langmuir*, 2006, **22**, 3830-3835.
- H.-S. Qian, S.-H. Yu, L.-B. Luo, J.-Y. Gong, L.-F. Fei and X.-M. Liu, *Chem. Mater.*, 2006, **18**, 2102-2108.
- H.-W. Liang, L. Wang, P.-Y. Chen, H.-T. Lin, L.-F. Chen, D. He and S.-H. Yu, *Adv. Mater.*, 2010, **22**, 4691-4695.
- A. Kuzume, E. Herrero and J. M. Feliu, *J. Electroanal. Chem.*, 2007, **599**, 333-343.
- M. D. Maciá, J. M. Campiña, E. Herrero and J. M. Feliu, *J. Electroanal. Chem.*, 2004, **564**, 141-150.
- N. Tian, Z.-Y. Zhou and S.-G. Sun, *J. Phys. Chem. C*, 2008, **112**, 19801-19817.
- T. Biegler, D. A. J. Rand and R. Woods, *J. Electroanal. Chem. Interfacial Electrochem.*, 1971, **29**, 269-277.
- A. Pozio, M. De Francesco, A. Cemmi, F. Cardellini and L. Giorgi, *J. Power Sources*, 2002, **105**, 13-19.
- X. Niu, C. Chen, H. Zhao, Y. Chai and M. Lan, *Biosens. Bioelectron.*, 2012, **36**, 262-266.
- Y. J. Lee, J. Y. Park, Y. Kim and J. W. Ko, *Curr. Appl. Phys.*, 2011, **11**, 211-216.
- P. Karam and L. I. Halaoui, *Anal. Chem.*, 2008, **80**, 5441-5448.
- J. Wang, *Chem Rev*, 2008, **108**, 814-825.

46. D. Zhai, B. Liu, Y. Shi, L. Pan, Y. Wang, W. Li, R. Zhang and G. Yu, *ACS Nano*, 2013, **7**, 3540-3546.
47. J. Liu, X. Wang, T. Wang, D. Li, F. Xi, J. Wang and E. Wang, *ACS Appl. Mat. Interfaces*, 2014, **6**, 19997-20002.